

## Experimental analysis of impact of MPPT methods on energy efficiency for photovoltaic power systems

Issam Houssamo, Fabrice Locment, Manuela Sechilariu\*

*Université de Technologie de Compiègne, AVENUES-GSU EA7284, BP 60319, rue du Docteur Schweitzer, 60203 Compiègne, France*

### ARTICLE INFO

#### Article history:

Received 1 August 2012

Received in revised form 15 October 2012

Accepted 20 October 2012

Available online 22 November 2012

#### Keywords:

Photovoltaic

Maximum power point tracking

Perturb and Observe

Incremental Conductance

Fuzzy Logic

Energy efficiency

### ABSTRACT

During recent years, for photovoltaic (PV) systems, many maximum power point tracking (MPPT) algorithms have been proposed and developed to maximize the produced energy. Regarding the design manner, these methods vary in many aspects as: implementation simplicity, power or energy efficiency, convergence speed, sensors required, cost effectiveness. Some comparative studies, based on widely-adopted MPPT algorithms, presented in the literature give results obtained either from simulation tool, which provide simultaneous operating systems, or using real PV test bench under solar simulator in order to reproduce the same operating solar conditions. This work presents an experimental comparison, under real solar irradiation, of four most used MPPT methods for PV power systems: Perturb and Observe (P&O) and Incremental Conductance, as tracking step constant, and improved P&O and Fuzzy Logic based MPPT, as variable tracking step. Using four identical PV, under strictly the same set of technical and meteorological conditions, an experimental comparison of these four algorithms is done. Following two criteria, energy efficiency and cost effectiveness, this comparison shows the advantage of use of a MPPT with a variable tracking step. The extracted energies by all four methods are almost identical with a slight advantage for improved P&O algorithm.

© 2012 Elsevier Ltd. All rights reserved.

### 1. Introduction

In recent years, the environmental problems become a worldwide issue. While the energy demand is significantly increasing against the decreasing reserves of fossil and fissile resources, the photovoltaic (PV) energy as an inexhaustible and clean source can reply to that demand. As one of distributed sources, the PV power is increasingly connected to the grid, either in large-scale and small-scale plants. Thus, the PV source must provide the maximum of its output power, and a maximum power point tracking (MPPT) method is used. MPPT algorithm enables to extract the maximum of power whatever the operating meteorological conditions, solar irradiance ( $g$ ) and PV cell temperature ( $\theta$ ). The PV panel has a non-linear characteristic curve ( $i-v$ ), which depend strongly on  $g$ . So, the output power-voltage characteristic ( $p-v$ ) is non-linear and depends also on  $g$ . Fig. 1 shows some curves ( $i-v$  and  $p-v$ ) of a Solar-Fabrik SF-130/2-125 PV panel, measured at  $\theta = 30^\circ\text{C}$  and under solar irradiance variation  $200 \text{ W/m}^2 \leq g \leq 600 \text{ W/m}^2$ . The PV cell temperature effect is less than the solar irradiance one. Each characteristic has only one point called maximum power point (MPP) defined by the maximum power point current  $i_{MPP}$  and maximum power point voltage  $v_{MPP}$ .

Through a converter, the impedance adjustment between the PV panel and the load is carried out, and the MPPT algorithm operates PV panel at MPP for providing the maximum power to the load as presented in Fig. 2.

Since the earliest MPPT method published in 1960s, we can count over than fifteen MPPT methods [1–4]. They can be classified following to MPP process seeking into indirect and direct method [4]. The indirect methods, such short-circuit and open-circuit methods, need a prior evaluation of the PV panel, or are based on mathematical relationships or database not valid for all operating meteorological conditions. So, they cannot obtain exactly the maximum power of PV panel at any irradiance and cell temperature. On the other side, the direct methods operate at any meteorological condition. The most used methods among them are: Perturb and Observe (P&O), Incremental Conductance (INC), and Fuzzy Logic (FL) based MPPT. Some direct MPPT can also be classified according to the method by which the command variable is changed. Thus, fixed-step MPPT algorithms and variable-step MPPT algorithms can be differentiated. According to the solar irradiance, homogeneous or not, there are some works that deal with the partial shading of the PV source [5,6]; however this case is not studied in current paper.

Another classification can be built based on the implementation simplicity, power or energy efficiency, convergence speed, sensors required, cost effectiveness. These criteria are often dependent to

\* Corresponding author. Tel.: +33 344234964; fax: +33 344235262.

E-mail address: [manuela.sechilariu@utc.fr](mailto:manuela.sechilariu@utc.fr) (M. Sechilariu).

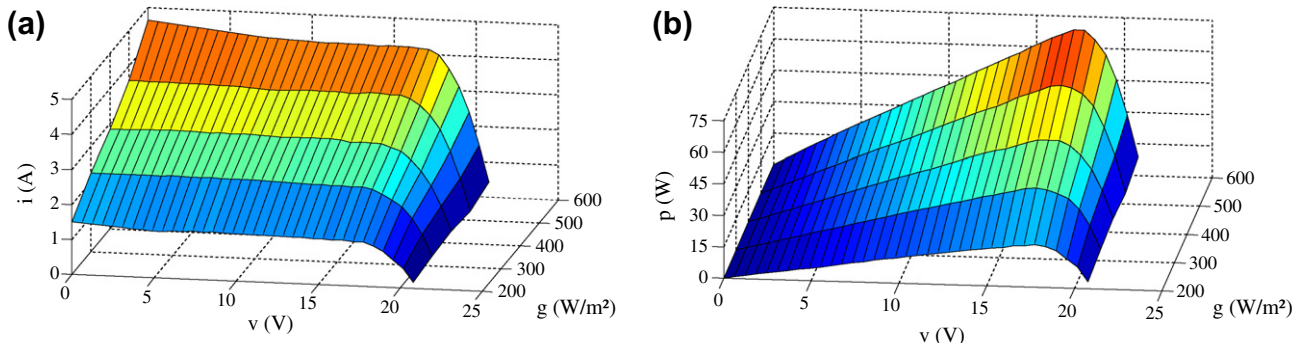


**Fig. 1.** Measured current–voltage and power–voltage characteristics of a SF-130/2-125 PV panel at  $\theta = 30^\circ\text{C}$ .

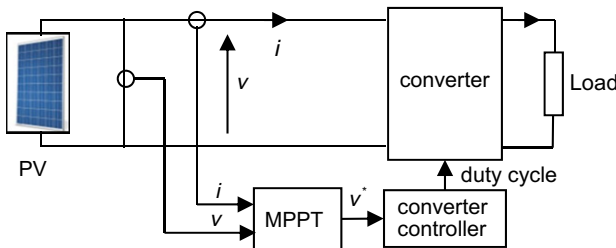


**Fig. 2.** Photovoltaic conversion based on impedance adapter controlled by MPPT algorithm.

each other, and make the choice of a MPPT method more difficult. Given the large number of studies on the MPPT algorithms in recent years, an analysis of the MPPT method, based on the more used ones, in both research and industrial applications, may clarify the MPPT position method over the chosen criteria and assist in decision making. Concerning the widely-adopted MPPT algorithms for PV systems, some comparative studies, presented in the literature give results obtained from simulation tool, which provide simultaneous operating systems. In the other hand, for real PV test bench, in order to reproduce the same operating solar conditions, comparative studies were done under solar simulator and often only for one PV panel.

So, this paper aims to meet the gap between simulation systems and experimental test under solar simulator, in order to compare four most used MPPT methods and to offer a decision support. On the other hand, the originality of this study lies also on experimental tests based on four identical PV power systems, under strictly the same set of technically and meteorological conditions. Finally, in this work, energy efficiency is emphasized by tests performed in situ and based on operation during 9 h while other studies use as main criterion the maximum power during few tens of seconds.

The principle criteria, which are taken into account for choosing the most suitable MPPT algorithm for PV power system, are maximum energy efficiency, calculation time, and simple implementation.

The paper is structured as follows. Two fixed-step tracking algorithms, P&O and INC, are presented and compared according the step size. Subsequently, two variable-step tracking algorithms are illustrated; the first one is an improved P&O (Imp&O) and the second one is an artificial intelligence method based on FL. Finally, the four methods are associated to four identical PV power systems and compared experimentally under strictly the same set of technical and meteorological conditions. According to two criteria, energy efficiency and cost effectiveness, and based on the experimental tests results, an analysis highlights the MPPT performances.

## 2. Fixed-step MPPT algorithms

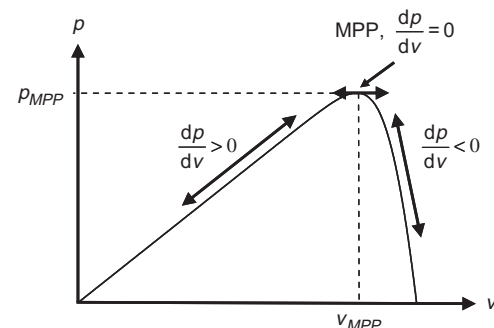
The most common fixed-step MPPT algorithms in both research works and industrial applications are P&O [7,8] and INC [9,10]. These algorithms operate in real time on the voltage reference variable corresponding to MPP of the PV power system.

### 2.1. Perturb and Observe algorithm

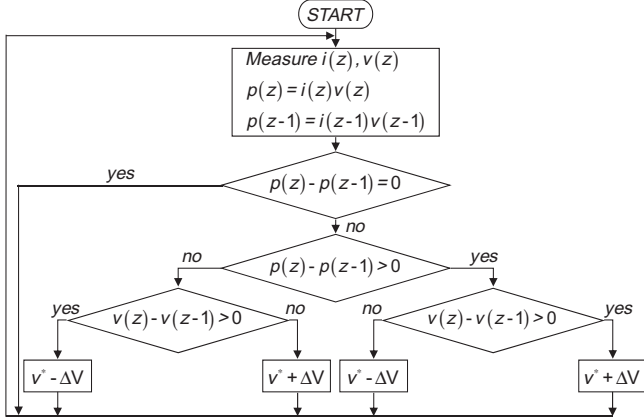
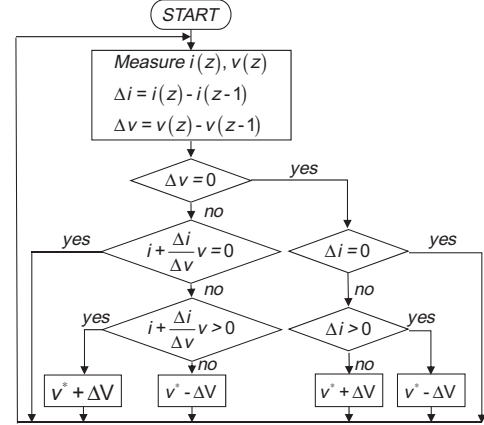
The P&O algorithm acts periodically by giving a perturbation to operating voltage  $v$  and observing the power variation  $p = vi$  in order to deduct the direction of evolution to give to the voltage reference  $v^*$ . Taking into account power–voltage characteristic curve  $p$ – $v$  obtained under given conditions ( $g, \theta$ ), the goal is to track the operating point at the MPP as shown in Fig. 3. This algorithm measures at each  $z$  instant the variables  $i(z)$  and  $v(z)$  and calculates  $p(z)$ , then compares with the power calculated at  $(z - 1)$  instant  $p(z - 1)$ .

For all the operating points where the power and current variations are positive, the algorithm continues to perturb the system in the same direction in increasing the voltage reference  $v^*$ , otherwise, if these variations are negative, the direction of perturbation is reversed. The increasing or decreasing of the reference  $v^*$  is done by the tracking step  $\Delta V$ . The flow chart of the P&O algorithm is presented in Fig. 4.

Theoretically, the algorithm is simple to implement in its basic form. However, it was noticed some oscillations around the MPP in steady state operating and this causes power loss [11]. Its functioning depends on the tracking step size applied to the voltage reference  $v^*$ . For the same sample time of the system, the oscillations, and consequently the power loss, could be minimized if the tracking step is continuously get smaller [12]. Nevertheless, the response of the algorithm becomes slower.



**Fig. 3.** Power–voltage characteristic of PV panel.

**Fig. 4.** Flow chart of the P&O algorithm.**Fig. 5.** Flow chart of the INC algorithm.

## 2.2. Incremental Conductance algorithm

In order to find out the position of the actual operating point in relation to MPP, this algorithm uses the derivate of the conductance  $di/dv$ . It is based on the fact that the slope tangent of the characteristic  $p-v$  is zero in MPP, positive on the MPP left side, and negative on the MPP right side, as illustrated in Fig. 3. As the power is equal to the product of current and tension, the calculation of this slope is given by:

$$\frac{dp}{dv} = \frac{d(vi)}{dv} = i + v \frac{di}{dv} \quad (1)$$

The development of this derivate in MPP is given by:

$$\frac{i}{v} + \frac{di}{dv} = 0 \quad (2)$$

When the operating point is located in the left side of the MPP, then  $i/v + di/dv > 0$ , whereas  $i/v + di/dv < 0$  when the operating point is on the other side. From the instantaneous measurement of  $i$  and  $v$ , the following approximations can be done:

$$\begin{cases} di \approx \Delta i = i(z) - i(z-1) \\ dv \approx \Delta v = v(z) - v(z-1) \end{cases} \quad (3)$$

So, the algorithm can instantly calculate  $i/v$  and  $di/dv$  to deduct the direction of the perturbation leading to the MPP. This is done by acting on  $v^*$ . Fig. 5 shows the flow chart of INC algorithm.

Concerning power efficiency, theoretically, this method could provide a better tracking of MPP than P&O algorithm [13]. However, due to the noise and error measurements, it seems interesting to note that experimentally Eq. (2) is never satisfied. It produces oscillations around the MPP and power loss. Furthermore, the complexity of INC algorithm, compared to P&O, increases the calculation time.

## 2.3. Considerations on P&O and INC

Maximum energy efficiency, calculation time, and simple implementation are the principle criteria taken into account in this paper for choosing the most suitable MPPT algorithm for PV power system.

P&O method has been highlighted in numerous studies in the literature to be less efficient than other methods, but on the basis of one criterion, to extract maximum power. However, this method, analyzed according to a criterion to extract maximum energy, is proved as effective as the INC. In the literature, comparisons between these two MPPT methods are not operated in technical and meteorological conditions strictly identical under real solar

irradiation. Based on the experimental platform installed on the roof of our university, tests were carried out in accordance with strictly identical real conditions, and thus the performance of these two fixed-step tracking MPPT algorithms was quantified by energy efficiency [13]. The comparison, based on three tests made at the same sample time, and three different fixed tracking steps, shows the influence of the tracking step value on the operation of MPPT algorithms. According to this work, it is concluded that P&O, when tracking step value is chosen correctly, can have an energy efficiency equivalent to that obtained with INC, while P&O is easier to implement compared with others MPPT methods.

## 3. Variable-step MPPT algorithms

This section proposes an improved P&O algorithm whose tracking step is variable following to the operating meteorological conditions. As one of the most common MPPT with variable-step tracking, the FL method is also studied in this section.

### 3.1. Improved Perturb and Observe algorithm

It is supposed an evolution of tracking step  $\Delta V$  according to characteristic slope  $dp/dv$  as shown in Fig. 6 (in red<sup>1</sup>). If the PV power system is near the MPP ( $|dp/dv| = 0$  or  $|dp/dv| \approx 0$ ), the tracking step oscillates between two values  $\Delta V_2$  and  $-\Delta V_2$ . This is why there are oscillations around the MPP which cause some power losses as previously mentioned. The performance of P&O can be improved by making the tracking step variable following the variations of operating conditions. The tracking step can vary according to the logic: if the PV power system is far away from the MPP ( $|dp/dv| > 0$ ), the tracking step must be large, otherwise it must be smaller. The same logic is used in [10] where the time variation of solar irradiation  $dg/dt$  is taken into account. The operating principle of the improved P&O (Imp&O) proposed in this paper is illustrated by the blue dashed line in Fig. 6.

So, if  $0 \leq |dp/dv| \leq |S_1|$ , the tracking step value is settled at  $\Delta V_1$ , while for  $|S_1| < |dp/dv| \leq |S_2|$  it vary linearly (is an arbitrary choice that we propose at this work stage). For  $|dp/dv| > |S_2|$ , the tracking step is settled at  $\Delta V_2$ , with  $\Delta V_2 > \Delta V_1$ .

As said at the beginning, to analyze the energy performance of the most used MPPT algorithms, a comparison according experimental tests is proposed. So, for consistency reasons, the value of  $\Delta V_2$  must be identical to the tracking step value used in fixed-step

<sup>1</sup> For interpretation of color in Figs. 1, 6–9, 10, 11, and 16–21, the reader is referred to the web version of this article.

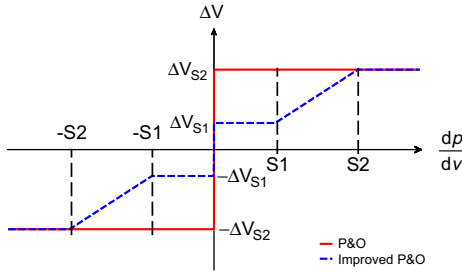


**Fig. 6.** Principle operation of P&O and ImP&O algorithms.

P&O and INC algorithms. Moreover, the value of  $\Delta V_{S1}$  and the thresholds  $S1$  and  $S2$ , must be well determined (empirical methods). Finally, based on the assumption that the variation of tracking step value between the thresholds  $S1$  and  $S2$  is linear, the implementation of ImP&O algorithm requires an iterative methodology and certainly some experience.

### 3.2. Fuzzy Logic MPPT

During recent years, the FL MPPT has used increasingly for the PV systems [13–17]. The FL MPPT can handle with imprecise inputs, works with the non-linear systems, and offers a robust control; however, the designer must have large knowledge and experience on PV system. The FL consists of mapping the input space and the output space through logical operations. The inputs/outputs are expressed as linguistic variables, called fuzzy sets, overlapped between each other. Using logical operations, the relationship is done between the input fuzzy sets and the outputs sets. Then, values are assigned to the outputs. This is why the design of FL MPPT requires experience and knowledge on PV power system operation. The FL MPPT generally consists of three stages: fuzzification, fuzzy reasoning and defuzzification.

#### 3.2.1. Fuzzification

During the fuzzification, the numerical values of the inputs/outputs are transformed into fuzzy sets. So, they are expressed in linguistic variables characterized by a membership called subset, which represents each point of input space or the universe of discourse. For a membership function, this is the matter of degree

rather than the value. Comparing with the Boolean logic in which the response is either 0 or 1, the degree of membership function takes many values between 0 and 1. Well designed FL MPPT satisfies every instant the equality  $dP/dV = 0$ , whatever the operating conditions. So, two inputs are taken into account,  $e_1 = dP/dV$  and  $e_2 = d(dP/dV)/dt$  which gives information about the direction and the rate of algorithm convergence toward the MPP, and the output is the tracking step  $\Delta V$  as shown in Fig. 7.

The FL MPPT is carried out by iterative methodology, so the two inputs are numerically defined by:

$$\begin{cases} e_1 = \frac{dP}{dV} = \frac{p(z) - p(z-1)}{v(z) - v(z-1)} \\ e_2 = e_1(z) - e_1(z-1) \end{cases} \quad (4)$$

The three fuzzy subsets that define the inputs and the output are illustrated in Fig. 8 as follow:  $e_1 \in \{\text{negative; zero; positive}\}$ ;  $e_2 \in \{\text{decreasing; stable; increasing}\}$ ;  $\Delta V \in \{-; 0; +\}$ , where the universe of discourse of the inputs and the output are  $[-100, 100]$  and  $[-1.75, 1.75]$ , respectively. In order to simplify this study, a triangular and trapezoidal membership functions were chosen instead of Gaussian or sigmoidal shapes.

The proposed FL MPPT design is considered enough accurate, but for more accuracy considerations some papers used five subsets as demonstrated [17].

#### 3.2.2. Fuzzy reasoning

Since the inputs and the output are fuzzified, mapping all the inputs with the output is known as fuzzy inference of fuzzy reasoning. This is accomplished using fuzzy “If-Then” rules [18]. The “If-Then” statement consists of two parts; the “If” part called antecedent and the “Then” part called the consequent. The antecedent defines a fuzzy region in the input space, while the consequent specifies the output in the fuzzy region. Table 1 summarizes the “If-Then” rules used in the proposed FL MPPT.

The fuzzy reasoning consists of two phases. The first one includes inputs fuzzifying and determination of the activated rules. The interpretation of the antecedent defines a region in the universe of discourse and returns values between 0 and 1, which are the values of the membership functions in that region.

The second phase of fuzzy reasoning seeks to determine the consequent of all activated rules and combining them. Firstly, a logical operator is applied to the membership functions values in

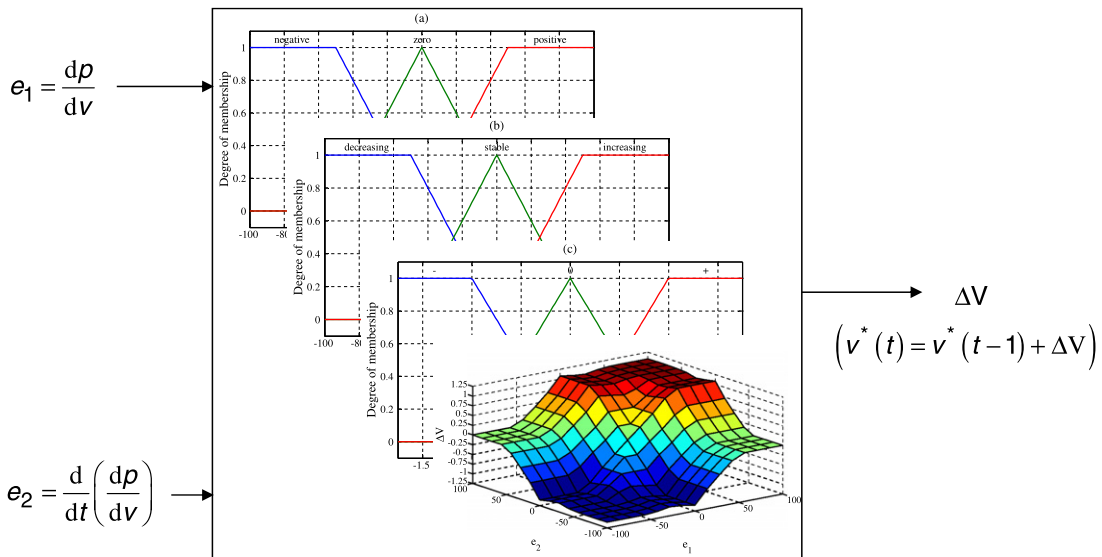


**Fig. 7.** Inputs and output of FL MPPT.

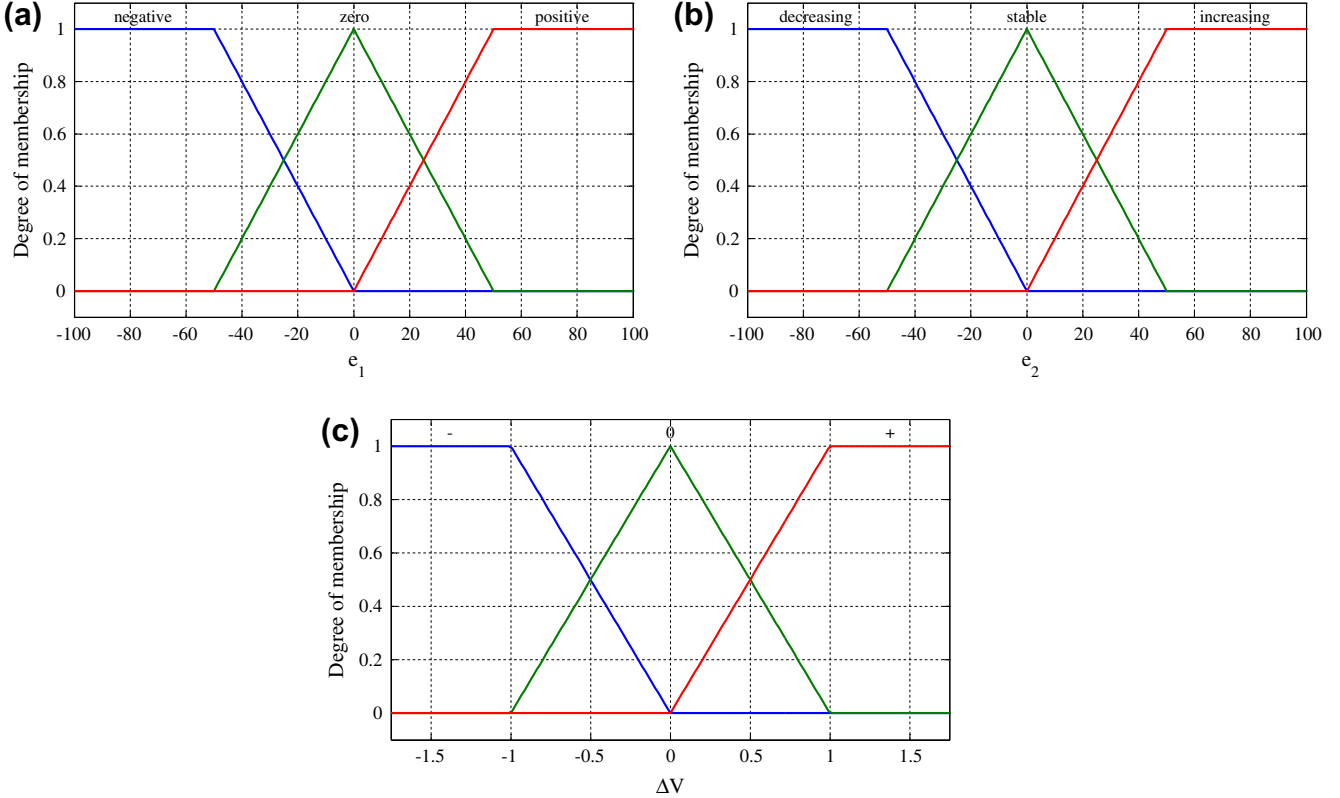


Fig. 8. Membership functions of inputs (a), (b), and of output (c).

**Table 1**  
Fuzzy rule table.

$\Delta V$		$e_2$		
		Decreasing	Stable	Increasing
$e_1$	Negative	—	—	0
	Zero	—	0	+
	Positive	0	+	+

order to evaluate the degree of each activated rule, which expresses how the antecedent part of each rule is satisfied. Then, the resulted number is used to determine the fuzzy sets in the consequent of each rule; this is called the “implication”. Finally, the fuzzy sets or the output of each rule are combined or aggregated

to form one fuzzy set. In this case study, one of the most common systems supported in MATLAB, fuzzy toolbox called Mamdani fuzzy inference system is used. It applies “And” (“min”) operation for evaluation of the activated rules degrees, and “Or” (“max”) for aggregating the fuzzy sets.

### 3.2.3. Defuzzification

The defuzzification main goal is to interpret the fuzzy set resulted from the aggregation into a numerical value to be used by the designer, i.e. the value of the tracking step  $\Delta V$ . Seven defuzzification operators are presented in [19], but the most used one is the centroid, or centre of gravity, computed generally by  $(\int \mu(\Delta V)\Delta V d(\Delta V) / \int \mu(\Delta V)d(\Delta V))$ , where  $\mu(\Delta V)$  is the degree of membership of the aggregated fuzzy set for the output  $\Delta V$ . If all

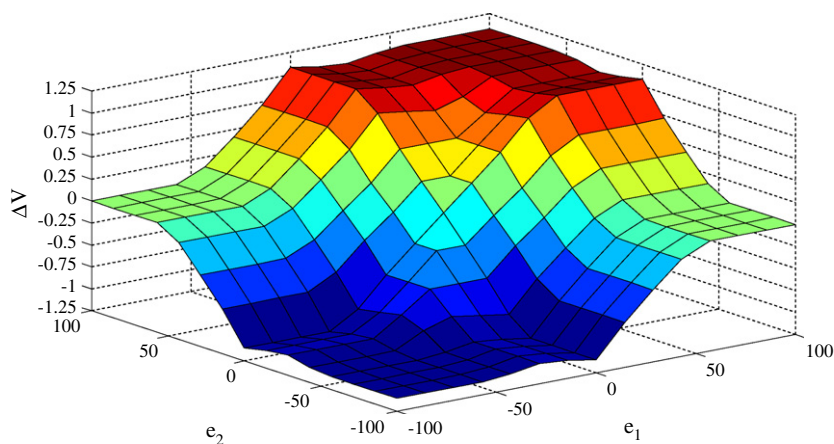
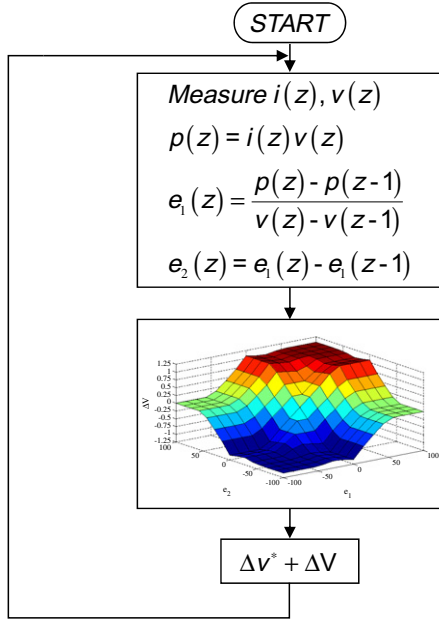


Fig. 9. Evolution of the output values  $\Delta V$  according to inputs  $e_1$  and  $e_2$ .

**Fig. 10.** Flow chart of FL MPPT.

the membership functions and “If–Then” rules are built, MATLAB fuzzy toolbox computes it for any input. The all output values  $\Delta V$  corresponding to the variation of the inputs  $e_1$  and  $e_2$  over the universe of discourse, is given in Fig. 9.

The flow chart shown in Fig. 10 summarizes the proposed FL MPPT.

#### 4. Experimental comparison of MPPT algorithms

Following two criteria, energy efficiency and cost effectiveness, in this section, the four above described MPPT algorithms are compared and their performance analyzed. In order to choose the most

suitable MPPT algorithm for PV power subsystem, the four methods are associated to four identical PV power system and compared experimentally under strictly the same set of technical and meteorological conditions. As this work is more focused at MPPT algorithms energy performance rather than at the control efficiency, a linear control is proposed and used.

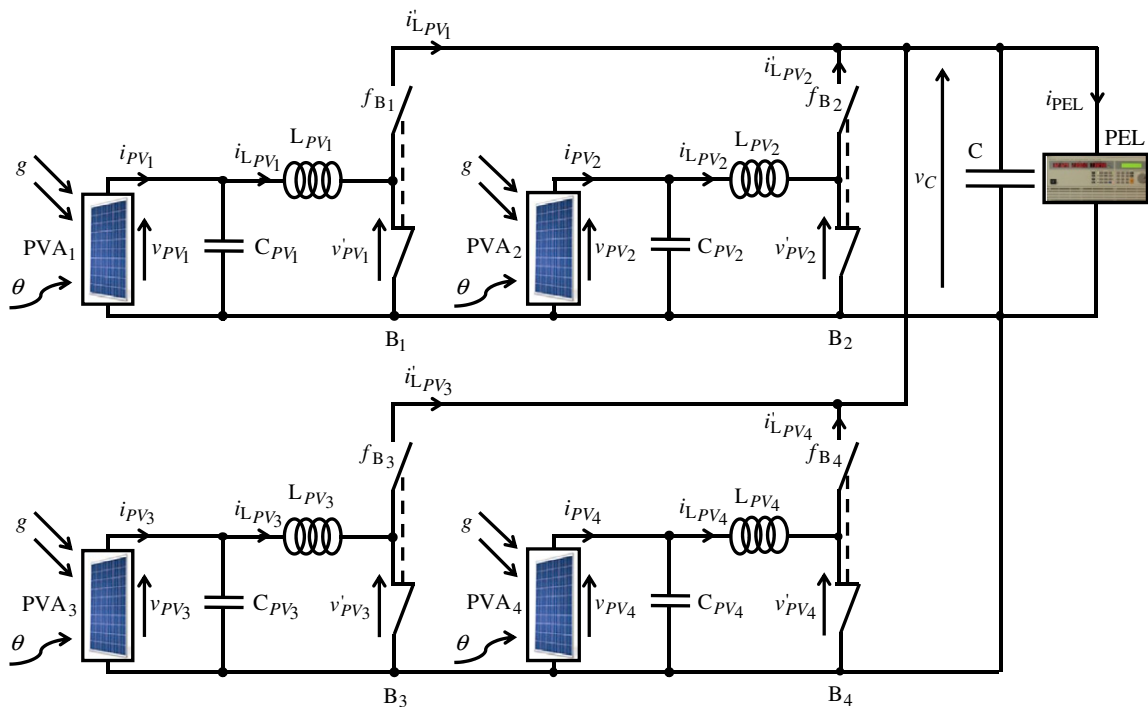
#### 4.1. Experimental system description

The experimental system is shown in Fig. 11. It is composed of four identical PV array (PVA) as  $PVA_N$  ( $N = 1, 2, 3, 4$ ); each one consists of four Solar-Fabrik SF-130/2-125 PV panels connected in series. All the  $PVA_N$  send the power to a DC voltage bus ( $v_C = 400$  V) through 4 legs ( $B_N$ ) of IGBT converter (SKM100GB063D) and a  $L_{PV_N} C_{PV_N}$  filter. The value of DC bus capacitor is  $C = 1100 \mu F$  and the filters elements have the following values: inductance  $L_{PV_N} = 10 mH$  with internal resistance (not shown in the figure)  $R_{PV_N} = 22.5 m\Omega$ , and the capacitor  $C_{PV_N} = 1000 \mu F$ . At the STC conditions, filters elements values allow to obtain the admissible voltage and current ripples. These values are also chosen within a reasonable cost. A programmable DC electronic load PEL (Chroma 63202, 2.6 kW) is used for dissipating the power produced by all the  $PVA_N$ .

#### 4.2. Converter control

As mentioned above, a linear control is implemented to each leg power converter  $B_N$ . There are two storage energy elements in each converter leg ( $L_{PV_N}$  and  $C_{PV_N}$ ). Thus, there are two states variables which are the PVA current and voltage  $i_{LPV_N}$  and  $v_{PV_N}$ . According to the first and second Kirchhoff laws, Eq. (5) given:

$$\begin{aligned}\frac{di_{LPV_N}}{dt} &= \frac{1}{L_{PV_N}} (V_{PV_N} - V_{PV_N} - R_{PV_N} i_{LPV_N}) \\ \frac{dv_{PV_N}}{dt} &= \frac{1}{C_{PV_N}} (i_{PV_N} - i_{LPV_N})\end{aligned}\quad (5)$$

**Fig. 11.** Experimental system.

Eq. (5) show that  $i_{L_{PV_N}}$  is a state variable and command variable,  $v_{PV_N}$  is a state variable and it is a disturbance at the same time,  $v'_{PV_N}$  is a command variable and  $i_{PV_N}$  is a disturbance. Based on these observations, the references  $i'_{L_{PV_N}}$  and  $v'_{PV_N}^*$  are obtained as in following equation:

$$\begin{aligned} i'_{L_{PV_N}} &= -C_V(v'_{PV_N} - v_{PV_N}) + i_{PV_N} \\ v'_{PV_N}^* &= -C_I(i'_{L_{PV_N}} - i_{L_{PV_N}}) + v_{PV_N} \end{aligned} \quad (6)$$

with  $C_V$  and  $C_I$  are respectively the voltage and current loops controllers. The modulated current and voltage are defined as follows:

$$\begin{bmatrix} i'_{L_{PV_N}} \\ v'_{PV_N} \end{bmatrix} = \alpha_N \begin{bmatrix} i_{L_{PV_N}} \\ v_C \end{bmatrix} \quad (7)$$

where  $\alpha_N$  represents the average values of switching functions  $f_{B_N}$  over one operating period  $T$  ( $\alpha_N = \frac{1}{T} \int f_{B_N} dt$ ,  $\alpha_N \in [0, 1]$ ). From Eqs. (6) and (7),  $\alpha_N^*$  can be determined:

$$\alpha_N^* = \frac{1}{v_C} (-C_V(v'_{PV_N}^* - v_{PV_N}) + i_{PV_N} - i'_{L_{PV_N}}) + v_{PV_N} \quad (8)$$

The Eq. (8) expresses a nested loop control, but the matter is to determine the controllers' values  $C_V$  and  $C_I$  for which the two loops will be uncoupled.

Fig. 12 shows a synoptic block-diagram of the used control, where  $\alpha_N$  is compared with a voltage carrier reference  $v_{REF}$  (triangle repeating sequence of 20 kHz frequency) in order to achieve PWM (Pulse Width Modulation), which determines the switching function  $f_{B_N}^*$ .

Regarding the correctors ( $C_V$  and  $C_I$ ), their structures must be chosen, and consequently their values determined. It is supposed that the command variables ( $v'_{PV_N}$  and  $i'_{L_{PV_N}}$ ) are slowly variable, capacitors  $C_{PV_N}$  are pure integrators, and inductances  $L_{PV_N}$  are first order systems. Controller  $C_V$  has to be at least a proportional corrector; however, as there is no real system pure, an integral controller may be added. So, PI (Proportional Integral) or IP (Integral Proportional) controller can be used. If the disturbance  $i_{PV_N}$  is correctly compensated, and if the converter is modeled by a unitary static gain, the voltage closed loop using an IP controller is illustrated in Fig. 13; where  $K_{1V}$  and  $K_{2V}$  are controller parameters.

From closed loop transfer function given by Eq. (9), the parameters  $K_{1V}$  and  $K_{2V}$  are defined as in Eq. (10).

$$\frac{v_{PV_N}}{v'_{PV_N}} = \frac{1}{1 + \frac{1}{K_{1V}} s + \frac{C_{PV_N}}{K_{1V} K_{2V}} s^2} = \frac{1}{1 + 2\zeta_V \tau_V s + \tau_V^2 s^2} \quad (9)$$

$$K_{1V} = \frac{1}{2\zeta_V \tau_V} \text{ and } K_{2V} = \frac{2\zeta_V C_{PV_N}}{\tau_V} \quad (10)$$

Depending on damping coefficient  $\zeta_V$ , time constant of closed loop  $\tau_V$ , and the value of capacitor  $C_{PV_N}$ , the parameters  $K_{1V}$  and  $K_{2V}$  are easily calculated. With a PI controller, the closed loop transfer func-

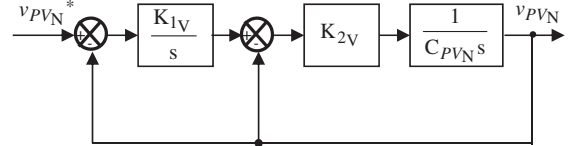


Fig. 13. Block-diagram of voltage closed loop.

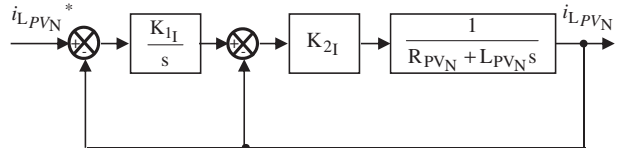


Fig. 14. Block-diagram of current closed loop.

tion includes two poles (real or complex conjugate) as well as one zero to be taken into account. So, the parameters tuning becomes more difficult. This is why we used an IP controller.

According to a similar reasoning, the proposed structure of the controller  $C_I$  is shown in Fig. 14. From the block-diagram of current closed loop, the transfer function and controller parameters are given by:

$$\begin{aligned} i'_{L_{PV_N}} &= \frac{1}{1 + \frac{K_{2I}}{K_{1I} K_{2I}} s + \frac{L_{PV_N}}{K_{1I} K_{2I}} s^2} = \frac{1}{1 + 2\zeta_I \tau_I s + \tau_I^2 s^2} \\ K_{1I} &= \frac{L_{PV_N}}{(2\zeta_I L_{PV_N} - \tau_I R_{PV_N}) \tau_I} \text{ and } K_{2I} = \frac{2\zeta_I L_{PV_N}}{\tau_I} - R_{PV_N} \end{aligned} \quad (11)$$

The values of parameters  $K_{1I}$  and  $K_{2I}$  are easily calculated depending on desired values of damping coefficient  $\zeta_I$ , time constant closed loop  $\tau_I$ , and the values of  $L_{PV_N}$  and  $R_{PV_N}$ .

Similarly to voltage loop, the PI controller brings a zero, but it may be easily eliminated in current loop by using dominant pole compensation method. Nevertheless, this method is not robust because the value of  $R_{PV_N}$  varies following the temperature, and the value of  $L_{PV_N}$  varies according to the saturation degree. For this reasons, an IP controller in the current loop is used.

The detailed synoptic block-diagram of the control proposed and implemented for MPPT comparison is shown in Fig. 15, where  $A_N$  refers to one of four tested MPPT algorithms.

Proper operation involves correct choice of the gains ( $K_{1V}, K_{2V}, K_{1I}$  and  $K_{2I}$ ), which requires satisfying of following inequalities:

$$\begin{aligned} \tau_V \gg \tau_I &\leftrightarrow \frac{1}{\omega_V} \gg \frac{1}{\omega_I} \leftrightarrow \frac{1}{2\pi f_V} \gg \frac{1}{2\pi f_I} \\ &\Rightarrow f_I \gg f_V \end{aligned} \quad (12)$$

with  $f_V$  and  $f_I$  the frequencies of voltage and current closed loops, respectively. Then, the dynamic of algorithm  $A_N$ , which imposes  $v_{PV_N}^*$ , must be lower than the other one of voltage loop.

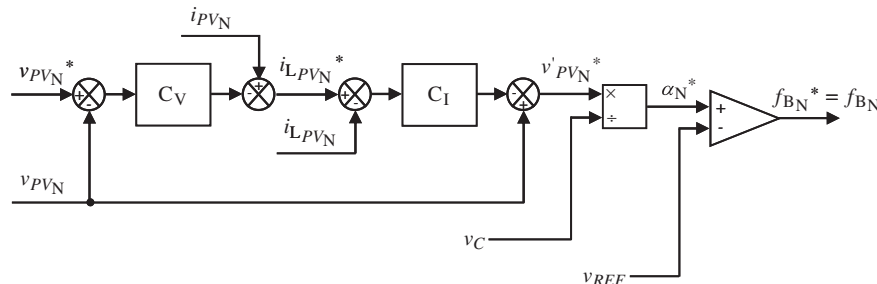
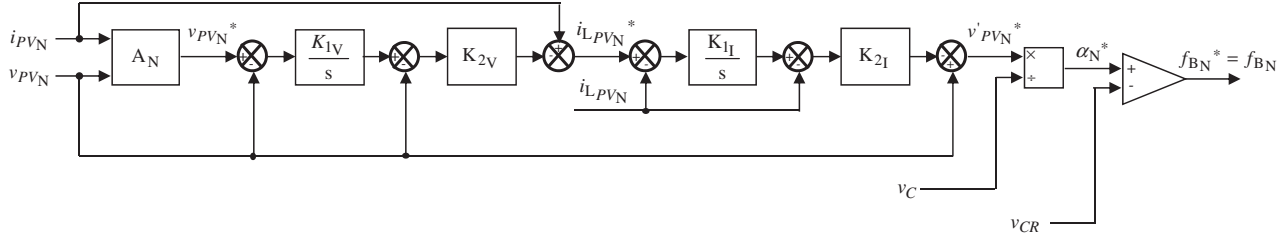


Fig. 12. Synoptic block-diagram of converter control.



**Fig. 15.** Detailed synoptic block-diagram of control used for MPPT study.

#### 4.3. Experimental results and analysis

Experimental 9-h continuous tests were operated in Compiegne, 2012, during the following days: April 3rd, 4th, 5th, 9th, 11th and 12th. The meteorological conditions in these days were different in both irradiance and temperature. Each MPPT algorithm is associated to a PVA<sub>N</sub>. The goal is to compare the described MPPT algorithms under the strictly same conditions ensured by the system structure described in Fig. 11.

The imposed sample time is 0.1 s for all algorithms. The damping coefficient for voltage and current loops is 0.707 ( $\zeta_V = \zeta_I = 0.707$ ) that leads to the best compromise between rapidity and precision. In order to satisfy the inequalities given by Eq. (12), the frequencies values of  $f_V$  and  $f_I$  are 5 Hz and 500 Hz, respectively.

The MPPT algorithms and the dedicated control are implemented in MATLAB-Simulink. The experimental system is controlled in real time by dSPACE 1103 with a sample time equals to 100  $\mu$ s (synchronized to the PWM at 20 kHz). The irradiance and temperature are respectively measured by a solar pyranometer CT-RM and temperature sensor PT100. During each test, the solar

irradiance ( $g$ ), air temperature ( $\theta_{AIR}$ ), cell temperature ( $\theta$ ), PVA current ( $i_{PV}$ ) and PVA voltage ( $V_{PV}$ ), are measured. The data acquisition is made by SL1000 (YOKOGAWA), which is also synchronized to the control of the dSPACE 1103 (100  $\mu$ s).

The PVA<sub>1</sub> and PVA<sub>2</sub> are respectively associated with P&O and INC algorithm, with following setting:  $\Delta V = 1$  V (which corresponds to a variation of  $\pm 10$  V/s). This value is estimated to be a good value, because it seems to work in almost all cases.

The ImP&O algorithm is implemented for PVA<sub>3</sub>, and the following settings are made:  $\Delta V_{S1} = \Delta V_{S2}/10 = 1/10 = 0.1$  V and  $S1 = S2 = 2$  W/V (values carried out from some tests).

The FL MPPT is associated with PVA<sub>4</sub>, the same parameters and settings shown in Section 3.2 are kept; however two scales factors are used (10 with the input  $e_1$ , and 1 with the input  $e_2$ ) to modify the inputs instead of the general profile.

Figs. 16–21 show the meteorological operation conditions (solar irradiance, air temperature and PV cell temperature) as well as the measured electrical power ( $p_{PVN} = v_{PVN} i_{PVN}$ ). The energies calculated using the trapeze method are given in Table 2.

For all tests days, the four algorithms operate in satisfactory manner. Given the matching with the measured power curve, the

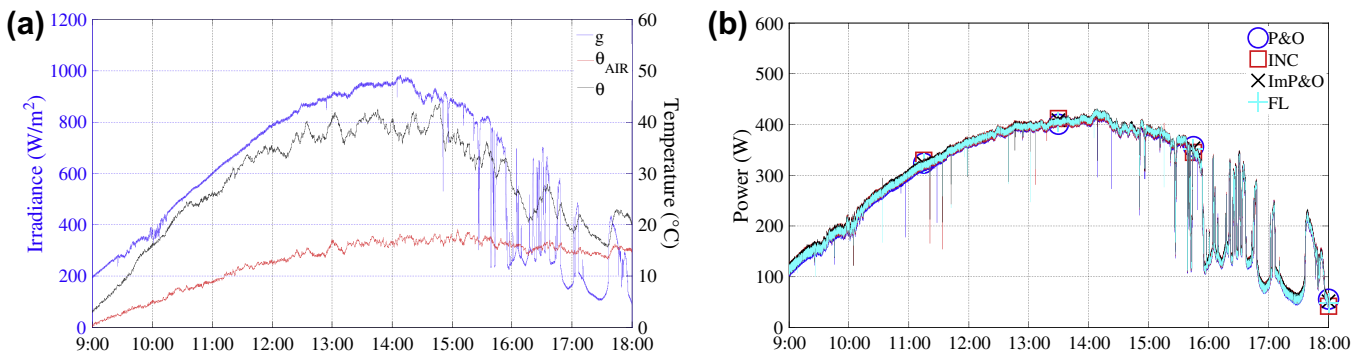


**Fig. 16.** Meteorological conditions (a) and electrical powers extracted (b) on 3rd of April 2012.

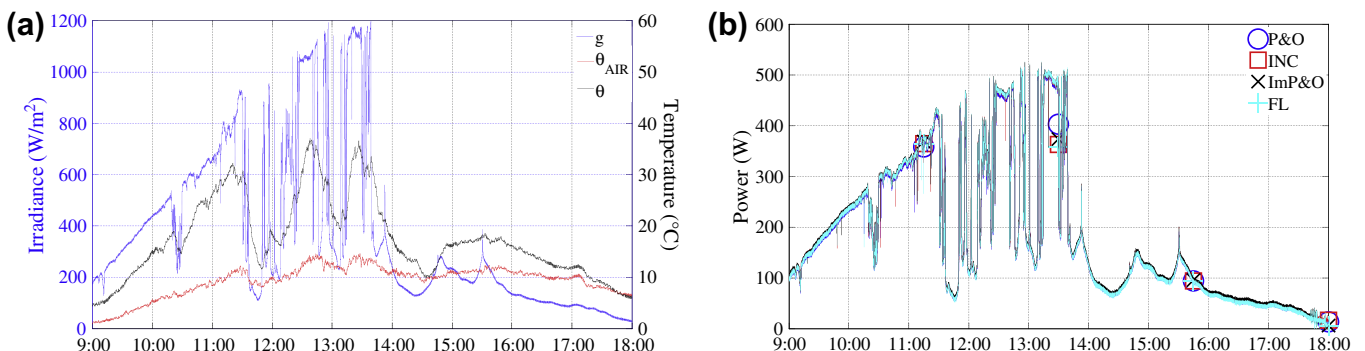


**Fig. 17.** Meteorological conditions (a) and electrical powers extracted (b) on 4th of April 2012.

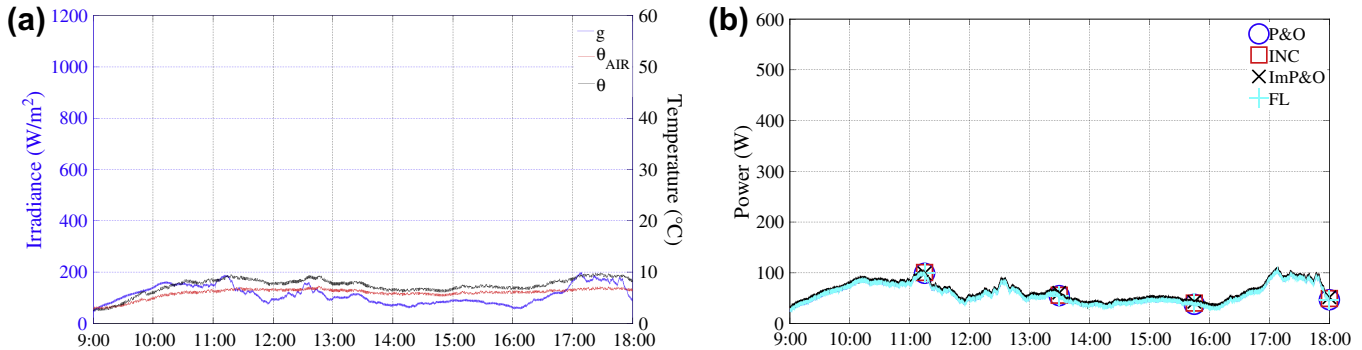


**Fig. 18.** Meteorological conditions (a) and electrical powers extracted (b) on 5th of April 2012.

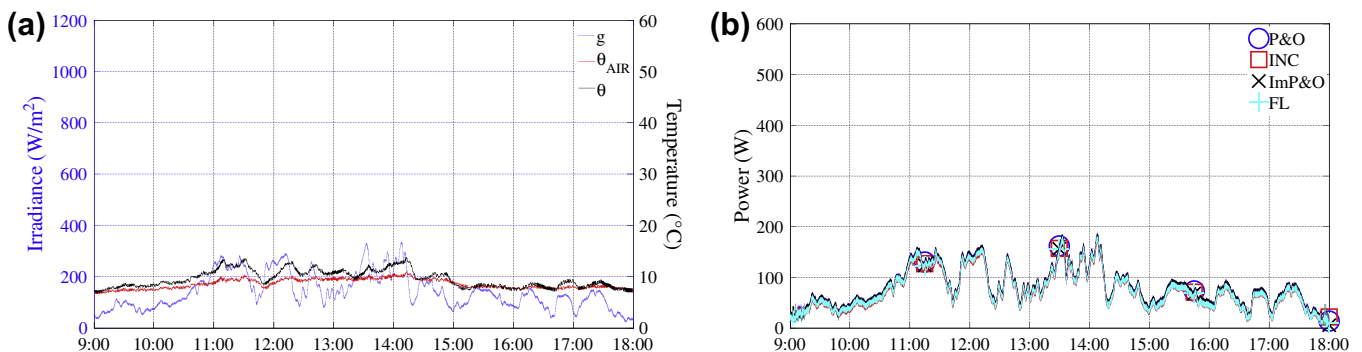


**Fig. 19.** Meteorological conditions (a) and electrical powers extracted (b) on 9th of April 2012.

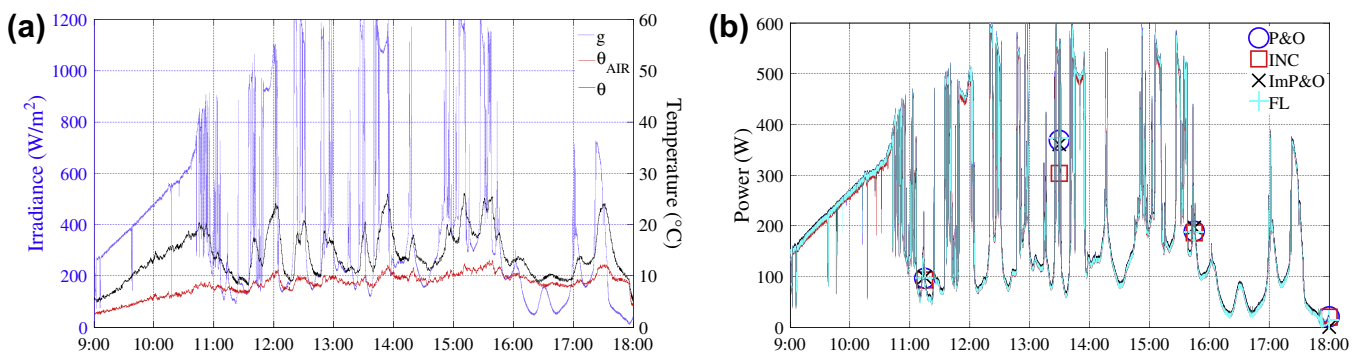


**Fig. 20.** Meteorological conditions (a) and electrical powers extracted (b) on 11th of April 2012.

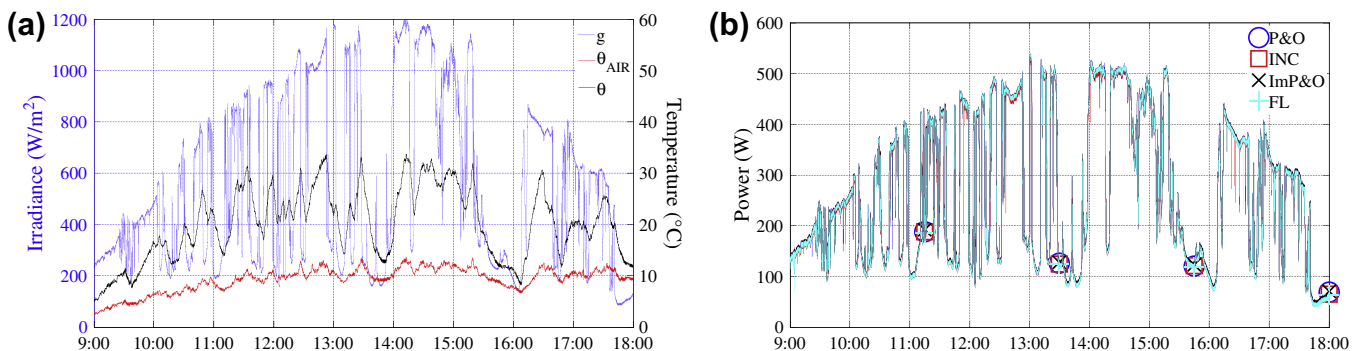


**Fig. 21.** Meteorological conditions (a) and electrical powers extracted (b) on 12th of April 2012.

**Table 2**

Extracted energies during experimental tests (kWh).

	April 3	April 4	April 5	April 9	April 11	April 12
P&O	2.53	1.59	0.53	0.68	1.73	2.36
INC	2.56	1.61	0.55	0.69	1.76	2.39
ImP&O	<b>2.57</b>	<b>1.63</b>	<b>0.57</b>	<b>0.71</b>	<b>1.79</b>	<b>2.41</b>
FL	2.55	1.6	0.53	0.68	1.76	2.38

**Table 3**

TOR of four extracted powers.

	April 3	April 4	April 5	April 9	April 11	April 12
P&O	19.67	21.14	<b>24.05</b>	43.17	40.53	23.99
INC	19.67	21.32	24.19	45.77	40.69	24.12
ImP&O	<b>10.07</b>	<b>21.07</b>	27.28	<b>19.16</b>	<b>38.71</b>	<b>23.86</b>
FL	10.69	22.1	32.01	22.31	40.53	24.67

figures show that four MPPT algorithms enable to extract almost the same power.

Table 2 shows that four MPPT algorithms extract almost the same energy; nevertheless the maximum of energy is extracted by ImP&O algorithm, as highlighted by bold values, and the minimum of energy is extracted by P&O algorithm. The relative errors between ImP&O and P&O vary from 1.56% (on 3rd of April) to 7% (on 5th of April). It is important to know that meteorological conditions as measured on 5th of April occur often in our region (North of France). Getting 7% of energy more is not negligible in measurement of energy performance. Otherwise, for very sunny days, as 3rd and 12th of April, which correspond to the highest extracted energy, the relative errors are small.

Regarding FL MPPT, it could not extract as much energy as INC algorithm or ImP&O algorithm. This poor performance may be due to improper adjustment of the scale factor of the input  $e_2 = d(dp/dv)/dt$ . Indeed, the derivate adjustment of another derivate is not so easy.

The extracted electrical power evolutions show that some algorithms induce power envelopes larger than others. In order to further analyze, the total oscillation rate, on each of the four electrical powers signals, was performed. Having a lot of points to be displayed, the graphical representation is not practical. So, the total oscillation rate (TOR) is calculated for each power, and the carried out results are given in Table 3 where the minimum TOR is evidenced by bold values. Except for April 5, Table 3 shows that the ImP&O algorithm causes less noise than the others three methods.

## 5. Conclusions

In this paper, four MPPT algorithms for PV power system are experimentally compared to select the best one in energy performance and implementation cost. Two fixed-step algorithms, P&O and INC, are explained. It is discussed that these algorithms may have some difficulties if the couple tracking step-sample time is incorrectly chosen. To overcome this drawback, improved MPPT methods with variable-step tracking are proposed and designed, ImP&O and FL MPPT.

Aiming to comparison under the strictly the same meteorological and technically conditions, the four MPPT algorithms, having consistency adjustment, are associated with four identical PVA coupled on a DC common bus through 4-leg power converter. The energy performance comparison, based on the measurement of four extracted powers, shows that the extracted energies are almost identical with a slight advantage for improved P&O algorithm. So, ImP&O algorithm optimizes the energy recovery

especially when solar irradiation is low. It enables also minimize the power oscillations. Consequently, ImP&O operates better than the others algorithms; in contrast, it requires know-how on PV power system operating.

Furthermore, following both criteria, energy efficiency and cost effectiveness, P&O has low cost effectiveness with very similar energy efficiency for long time period. Although the ImP&O method has the greatest energy efficiency, this does not justify the higher implementation cost, unless if required for specifically research works. For PV industrial applications, where the economic criterion is the most important one, this work proves the effectiveness of P&O, while it is claimed in the literature to be inferior to others MPPT methods. Also, this study justifies the most widely used MPPT method in industrial applications faced to others algorithms.

## Acknowledgements

This work is supported by the research funds of Conseil Régional de Picardie (CRP) France and European Union (FEDER), funds allocated to the Project GEO-ECOHOME (2011–2014).

## References

- [1] Esram T, Chapman PL. Comparison of photovoltaic array maximum power point tracking techniques. *IEEE Trans Energy Convers* 2007;22(2):439–49.
- [2] Irmak E, Güler N. Application of a high efficient voltage regulation system with MPPT algorithm. *Int J Electr Power Energy Syst* 2013;44(1):703–12.
- [3] Kassem AM. MPPT control design and performance improvements of a PV generator powered DC motor-pump system based on artificial neural networks. *Int J Electr Power Energy Syst* 2012;43(1):90–8.
- [4] Salas V, Olias E, Barrado A, Lazaro A. Review of the maximum power point tracking algorithms for stand-alone photovoltaic systems. *Sol Energy Mater Sol Cell* 2006;90(11):1555–78.
- [5] Chowdhury SR, Saha H. Maximum power point tracking of partially shaded solar photovoltaic arrays. *Sol Energy Mater Sol Cell* 2010;94(9):1441–7.
- [6] Ramaprabha R, Balaji M, Mathur BL. Maximum power point tracking of partially shaded solar PV system using modified Fibonacci search method with fuzzy controller. *Int J Electr Power Energy Syst* 2012;43(1):754–65.
- [7] Bianconi E, Calvente J, Giral R, Mamarelis E, Petrone G, Ramos-Paja CA, et al. Perturb and observe MPPT algorithm with a current controller based on the sliding mode. *Int J Electr Power Energy Syst* 2013;44(1):346–56.
- [8] Sera D, Kerekes T, Teodorescu R, Blaabjerg F. Improved MPPT algorithms for rapidly changing environmental conditions. In: Proceedings of 12th international power electronics and motion control conference; 2006. p. 1614–9.
- [9] Locment F, Sechilaru M, Houssamo I. DC load and batteries control limitations for photovoltaic systems experimental validation. *IEEE Trans Power Electron* 2012;27(9):4030–8.
- [10] Peftitis D, Adamidis G, Balouktsis A. An investigation of new control method for MPPT in PV array using DC – DC buck – boost converter. In: Proceedings of 2nd WSEAS/IASME international conference on renewable, energy sources; 2008.
- [11] Tafticht T, Agbossou K, Doumbia ML, Chériti A. An improved maximum power point tracking method for photovoltaic systems. *Renew Energy* 2008;33(7):1508–16.
- [12] Locment F, Sechilaru M, Houssamo I. Energy efficiency experimental tests comparison of P&O algorithm for PV power system. In: Proceedings of international power electronics and motion control conference; 2010.
- [13] Houssamo I, Locment F, Sechilaru M. Maximum power tracking for photovoltaic power system: development and experimental comparison of two algorithms. *Renew Energy* 2010;35(10):2381–7.
- [14] Gounden NA, Ann Peter S, Nallandula H, Krishiga S. Fuzzy logic controller with MPPT using line-commutated inverter for three-phase grid-connected photovoltaic systems. *Renew Energy* 2009;34(3):909–15.
- [15] Viswanathan K, Oruganti R, Srinivasan D. Nonlinear function controller: a simple alternative to fuzzy logic controller for a power electronic converter. *IEEE Trans Ind Electron* 2005;52(5):1439–48.
- [16] Mazouz N, Midoun A. Control of a DC/DC converter by fuzzy controller for a solar pumping system. *Int J Electr Power Energy Syst* 2011;33(10):1623–30.
- [17] Algazar Mohamed M, AL-monier Hamdy, EL-halim Hamdy Abd, Salem Mohamed Ezzat El Kotb. Maximum power point tracking using fuzzy logic control. *Int J Electron Power Energy Syst* 2012;39:21–8.
- [18] Yadav OP, Singh N, Chinnam RB, Goel PS. A fuzzy logic based approach to reliability improvement estimation during product development. *Reliab Eng Syst Safe* 2003;80:63–74.
- [19] Sumathi S, Surekha Panneerselvam. Computational intelligence paradigms. Theory and applications using MATLAB. Boca Raton: CRC Press; 2010.